Cement & Concrete Composites 32 (2010) 611–616

Contents lists available at ScienceDirect

Cement & Concrete Composites

journal homepage: www.elsevier.com/locate/cemconcomp

Effects of distribution of lightweight aggregates on internal curing of concrete

Burcu Akcay [a,*], Mehmet Ali Tasdemir [b]

[a] University of Kocaeli, Department of Civil Engineering, Izmit 41380, Turkey
[b] Istanbul Technical University, Civil Engineering Faculty, Maslak 34469, Istanbul, Turkey

ARTICLE INFO

Article history:
Received 9 February 2008
Received in revised form 16 June 2010
Accepted 6 July 2010
Available online 11 July 2010

Keywords:
Autogenous shrinkage
Internal curing
Lightweight aggregate
Image analysis

ABSTRACT

This study investigates the effects of spatial distribution of lightweight aggregates (LWAs) on internal curing of concrete. As replacements for normal aggregates, different sizes and amounts of natural pumice LWAs were used as water reservoirs to provide internal curing in mitigating autogenous deformation. Water in the pre-soaked LWAs flows into cement paste during hydration and provides internal curing to counteract the RH loss due to self-desiccation of binding paste. The results show that variations in the autogenous strain of concrete can be evaluated in terms of LWA–LWA proximity. The protected paste volume approach, previously used for air-entrained concrete, is applied to calculate the internally-cured volume of paste. The results show that the experimental rate of mitigation of autogenous strain for different series of concrete specimens, with respect to the reference concrete, gave the best-fitted values at water flow distance of 1 mm. The results indicate that the protected paste volume in internal curing can be determined by calculating the water-entrained volume using image analysis.

1. Introduction

Autogenous shrinkage can cause early age cracking of cement based materials, and this has generated considerable interest in this subject. Recent studies have shown that there are a number of methods that can mitigate autogenous deformation [1–11]. These include using shrinkage reducing admixtures [1,2], expansive additives [1,3], or slower reacting silica fume [4]; or internal curing (with lightweight aggregates (LWAs), superabsorbent polymers [5], recycled aggregates [6], or wood derived powders and fibers [7]). As another method, specific cement composition, such as Portland cement containing higher C_2S (belite) content [8], can be altered to minimize the effects of autogenous deformation. In addition, to prevent early age cracking due to autogenous shrinkage, fibers can be used to enhance the tensile strain capacity of cement paste [9–11].

Among these, internal curing is one of the most effective as it supplies water to the cementitious binder, which helps to keep the pore network saturated. Autogenous deformation will be mitigated only within the water-entrained volume through which the LWA can release water into the cement paste [5,12]. As a consequence, if the water can travel through the cement paste easily, internally-cured volume increases. The efficiency of internal curing is therefore affected by the distribution of LWAs, as well as the size and volume of LWAs.

This study aims to investigate the effects of distribution of LWAs on internal curing of concrete in mitigating autogenous strain. For this purpose, the flow distance of water from LWAs into the cement paste has been investigated by image analysis and this distance has been used for determining the protected paste volume. Then, dispersion characteristics of LWAs and their effects on the internal curing have been determined by image analysis. The distribution of reservoirs and the water flow into cement paste have been investigated in a manner similar to that in air-entrained concrete. In the protected paste volume concept, the fraction of the cement paste within a given distance of LWA is determined, and the spacing equations of LWAs are identified.

2. Water flow from LWA to the cement paste

In order to demonstrate the water flow from LWA to cement paste, the solution with red concrete colored pigment was used (Fig. 1a). Artificial expanded clays with spherical surfaces were mixed with white cement after 1-day absorption of pigmented water (w/c = 0.28). Then, microphotos were taken around the surface of LWA using high-resolution cameras. The images were adjusted using color histogram equalization. To have a better view, the images were inversed; hence the microphoto of water flow from LWA into the cement paste is obtained (the blue rim) as shown in Fig. 1b. Although water with pigments has a different surface tension compared to normal water, the flow distance of water from the outer surface of LWA to the cement paste was determined as 100 μm at 24 h [13], but increased to 1 mm in

* Corresponding author. Tel.: +90 262 3033270; fax: +90 262 3033003.
E-mail address: burcu.akcay@kocaeli.edu.tr (B. Akcay).

0958-9465/$ - see front matter © 2010 Elsevier Ltd. All rights reserved.
doi:10.1016/j.cemconcomp.2010.07.003

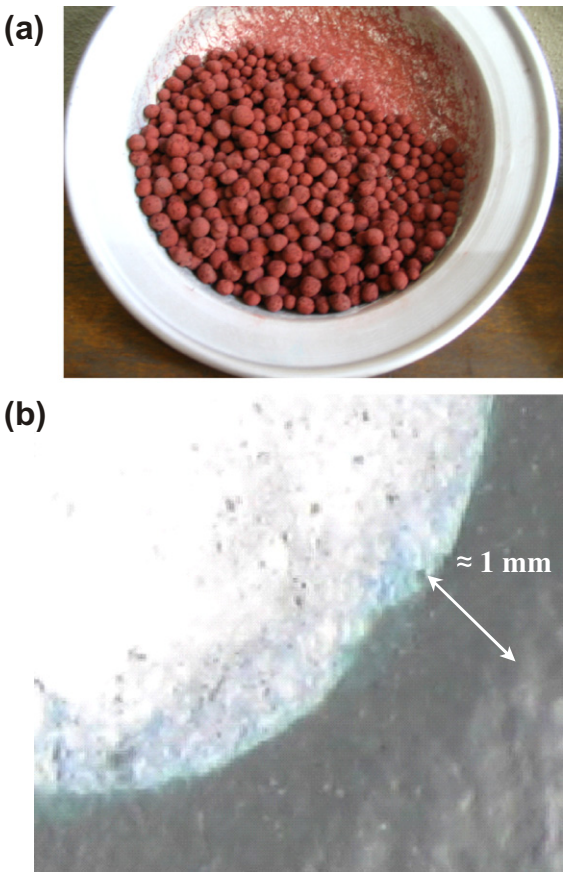

Fig. 1. (a) Expanded clays saturated with concrete colored pigment solution; (b) image showing the water flow from LWA to cement paste.

3 days. Similar results were also obtained by some other recent studies [14], suggesting that LWA can release water from its outer surface into the cement paste with a thickness of approximately 1 mm. It is clear, however, that this value is dependent on the size and pore structure of LWA as well as the pore structure of cement paste.

The tests were also repeated for the age of 7 and 28 days after casting. The results show that no time dependent change in the water flow distance is observed for these ages, although some researchers argue that the thickness of water flowed rim varies significantly with time and suggest that penetration of water from LWA into the cement paste is dependent on the permeability of cementitious materials [12]. The water cannot effortlessly move through into the concrete with the increasing degree of hydration. Bentz et al. [12] stated that flow distances vary from tens of millimeters at early ages to millimeters at middle ages to hundreds of micrometers at later ages. It is, however, obvious that this distance is affected by a number of factors including w/c ratio, cement content and type, and pore structures of LWA. The results obtained from this study indicate a water flow distance of only 1 mm at 3, 7, and 28 days for cement paste with w/c of 0.28, although this distance for concrete samples may be greater than 1 mm. It should be noted that, however, the binding of red pigments to the matrix may slow down the movement of pigment in later ages.

3. Experimental details

To examine the effects of size and volume of LWAs on autogenous deformation of concrete, seven concretes were prepared using constant water to binder ratio of 0.28 with addition of 10% silica fume (by cement weight) and a constant aggregate volume of 65%. An ordinary Portland cement (OPC 42.5) was used in all concretes with a Blaine fineness of 3280 cm^2/g and an estimated Bogue composition of 57% C_3S, 17% C_2S, 5% C_3A, 11% C_4AF (by mass fraction). Particle densities of crushed limestone, crushed sand, quartz sand, and siliceous powder were 2720, 2710, 2650 and 2620 kg/m^3, respectively. Normal aggregates were replaced by natural LWAs with size fractions of 2–4 mm or 4–8 mm at three different volume fractions such as 10%, 20%, and 30% of the total aggregate volume of concrete. Natural pumice from the Capadocia area, Central Turkey, was used as lightweight aggregate. Fine and coarse pumice LWAs have particle densities (24-h saturated surface dry condition) of 1070 and 1020 kg/m^3, respectively. Presoaked water contents, which were determined using the 30 min water absorption, were found to be 35% and 33% for fine and coarse LWAs, respectively.

The mixture design, codes, and some of the fresh properties of the concretes are given in Table 1. The numbers following the letter V and L in the designation code denote replacement volume and the replaced size fraction of LWAs, respectively. Exception, however, is the reference concrete (CREF) which contains normal weight aggregate only.

The linear autogenous deformations of concretes were determined by measuring displacements on the sealed prism specimens of 70 × 70 × 280 mm. Stainless steel studs were settled on specimens using a thin layer of adhesive after initial setting time of approximately 4 h and the side walls were de-moulded. The measurements were taken over 200 mm gauge length (with an accuracy of 0.001 mm/m) according to the ASTM C 41.

The detailed discussion on the result of the autogenous strain of the concretes can be found in another paper of the same authors, in which optimum size and content of LWAs were established for more ductile concrete with less autogenous strain using a multi-

Table 1
Compositions and properties of the fresh mixtures (for 1 m^3).

Composition of concrete in 1 m^3													Fresh properties
Code	Binder		Liquid			Aggregate							Unit weight, kg/m^3
	Cement, kg	Silica fume, kg	Water, kg	Pre-soaked water, kg	Superplasticizer, kg	Siliceous powder, kg	Natural sand (0–2), kg	Crushed coarse sand (2–4), kg	Crushed stone (4–8), kg	LWA 2–4 mm, kg	LWA 4–8 mm, kg	Air, %	
CREF	497	50	153	0	10	169	514	520	529	0	0	1.4	2442
CV10L24	496	50	153	17	10	169	513	344	529	48	0	1.5	2329
CV10L48	497	50	153	34	10	169	513	520	353	0	47	1.3	2345
CV20L24	496	50	153	51	10	169	513	173	529	97	0	1.2	2241
CV20L48	497	50	153	16	10	169	514	520	177	0	94	1.2	2200
CV30L24	496	50	153	31	10	169	513	0	528	145	0	1.3	2095
CV30L48	496	50	153	47	10	168	512	519	0	0	141	1.4	2096

objective simultaneous optimization technique [17]. Here, brief information regarding the experimental results is given before presenting the main topic of the paper, the distribution of LWAs, and evaluating the results.

The linear autogenous shrinkage strain results of concretes are shown in Fig. 2. The replacement of normal aggregate by fine fraction of LWA was shown to be more effective in reducing the autogenous strain compared to the use of coarse fraction of LWAs. While the linear autogenous strain of reference concrete (CREF) was −537 microstrain (l μm/m) at 28 days, this value was mitigated with using fine LWAs by 24%, 47% and 92%, for replaced volume fractions of 10%, 20% and 30%, respectively. On the other hand the use of coarse LWAs mitigated autogenous strain by 11%, 32% and 65% at the same volume fractions. As it can be seen both size and volume of LWAs dominates the internal curing. In the following section the effects of distribution of these water reservoirs on mitigation ratios of autogenous shrinkage will be discussed.

To find out whether the LWAs have effects on autogenous shrinkage of cement paste other than internal curing, the supplementary test series were conducted. The cement paste sample was prepared using the water/cement ratio of 0.28 (without addition of silica fume), while another test sample was prepared replacing 30% by volume of reference cement paste using expanded clays (with particle size fractions of 4.00–6.73 mm) saturated with water for 30 min. In the third series, all artificial expanded clay LWAs were coated by a thin layer of paraffin one by one to obstruct the water flow. All the autogenous deformation were tested in volumetric measurements and duplicated.

The normalized results regarding the cement paste content are shown in Fig. 3 where the autogenous strain of the cement paste with coated LWAs resembles to that of the plain cement paste. On the other hand, the cement paste, in which the water flow from LWAs to the paste is allowed, displays significantly lower magnitude of autogenous strain, which is consistent with the known fact

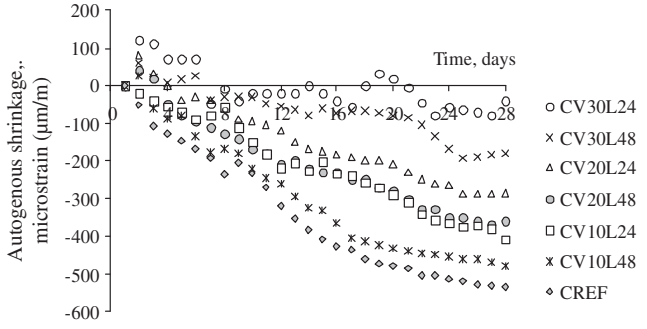

Fig. 2. Effects of size and volume of pre-soaked LWAs on linear autogenous strain of concretes.

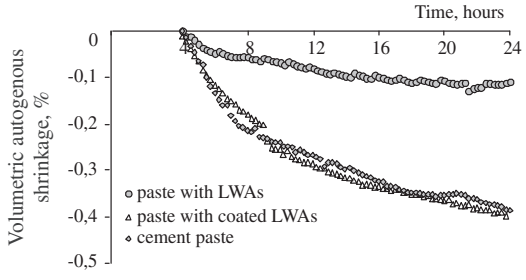

Fig. 3. Volumetric autogenous shrinkage versus time diagram for plain cement paste, cement paste with expanded clays samples and paste containing paraffin coated expanded clays.

that LWAs reduce the autogenous deformation by releasing water to media (Fig. 3). Since the LWAs used in these tests have relatively lower modulus of elasticity (approximately 5000 MPa [15,16]), they cannot restrain the shrinkage of cement paste significantly.

4. Spatial distribution of LWAs

The spatial distribution of LWAs can be considered similar to the distribution of air voids in air-entrained concrete. For air-entrained concrete there are mainly two types of spacing definitions; paste–void proximity and void–void proximity. Paste–void proximity equations estimate the volume fraction of paste within some distance from the surface of the nearest air void. When the size and volume fraction of LWAs is known, the water release distance from LWAs can be used to determine the water-entrained volume fraction of cement paste. The void–void proximity can be examined in two different ways as the nearest neighbor and mean free path calculations [18]. The nearest neighbor void–void proximity equations are based on the calculation of distance from the surface of air voids to the surface of the nearest neighbor air void. The other definition of void–void proximity, the mean free path, is a numerical expression rather than a distribution. It is defined as the average length of paste between the closest air voids along an arbitrarily selected line, similar to the chord length given in ASTM C 457.

There are a number of spacing factors defined to estimate the paste–void proximity such as the definitions of Powers [19], Philleo [20], Pleau and Pigeon [21], Lu and Torquato [22]. The equations for void–void proximity have been derived by a number of authors (e.g. Lu and Torquato [22] and Attiogbe [23,24]).

The paste–void or void–void distances can be identified by their cumulative distribution function (CDF) and probability density function (PDF). Since there is not any single theoretical value defined for the spacing, following the approach by Snyder [18], the 50th and the 95th percentiles of the spacing distributions were taken here as representing the quantity of spacing. As the water flow from LWAs into cement paste is conceptually similar to the air-entrained concrete [25,26], the distribution of water reservoirs will be defined as the distribution of air voids in air-entrained concrete.

4.1. Application for internal curing

In the light of above definitions and results, for the replacement of 10%, 20%, 30% volume and 2–4 mm and 4–8 mm size fraction of LWAs, the nearest surface distribution of LWAs were found by the image analysis on the pieces of broken beam specimens. The surfaces examined were first gently smoothed and cleaned. The images were obtained by high-resolution camera and then processed by image analysis programs. The images, in which the pumice LWAs can be easily distinguished with their white colors (Fig 4a), were made binary as shown in Fig. 4b. In addition, it is found from the images shown in Fig. 4 that LWAs can be well fitted to ellipses rather than circles.

In order to calculate the protected paste volume, the volume of the cement paste was first calculated. The ellipses were then enlarged using the possible flow length of water as 0.5, 1, and 2 mm, and then the volume of the cement paste and the protected volume of cement paste were recalculated. In calculations, it was assumed that the normal aggregates were in water-saturated conditions, which means that water for internal curing was not absorbed by normal aggregates.

For the calculations of LWA–LWA proximity distribution, the image area was first divided into parallel lines with a distance of 10 mm, and then the nearest neighborhoods of LWAs for each line were obtained. The parallel lines were then rotated up to 90° with

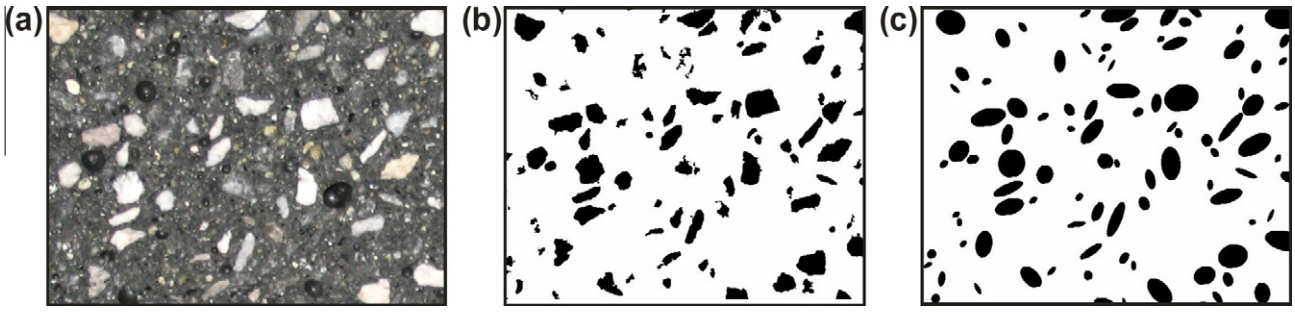

Fig. 4. (a) Real image of concrete, (b) LWAs in binary image of concrete, (c) ellipses fitting to LWAs. It is shown that there is only a small number of particles with circular geometries.

15° intervals. For each interval, analysis of the nearest neighbor distance of LWAs was repeated as shown in Fig. 5.

In addition, Powers and Attiogbe mean spacing factors were also determined to provide a comparison with the above calculated results. The Powers spacing factor $\bar{L}$, for paste-LWA proximity, was calculated using the following equation [19]:

$$\bar{L} = \begin{cases} \frac{p_v}{\alpha_v A_v}, & p_v/A_v < 4.342 \\ \frac{3}{\alpha_v}\left[1.4\left(\frac{p_v}{A_v}+1\right)^{1/3}-1\right], & p_v/A_v \geqslant 4.342 \end{cases} \quad (1)$$

where A_v is the LWA volume fraction, p_v is the paste volume fraction, and α_v is the specific surface area of LWAs.

Attiogbe mean spacing factors, which were originally defined for void–void proximity in air-entrained concrete, were used to calculate the LWA–LWA proximity. Attiogbe defined two different spacing, which are termed here as $\bar{s}_1$ and $\bar{s}_2$ with the following equations [23,24]:

$$\bar{s}_1 = 2\frac{p_v^2}{\alpha_v A_v} \quad (2)$$

$$\bar{s}_2 = 2F_v\frac{p_v^2}{\alpha_v A_v} \quad (3)$$

$$F_v = \frac{8}{p_v/A_v + 1} \leqslant 1 \quad (4)$$

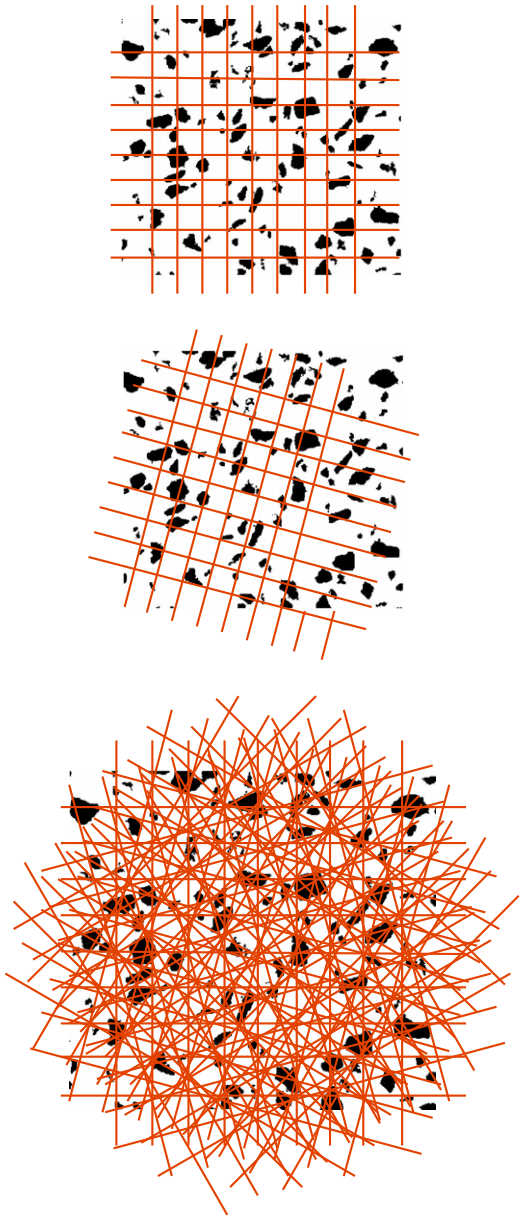

Fig. 5. Calculation steps for nearest distance of LWA–LWA surfaces.

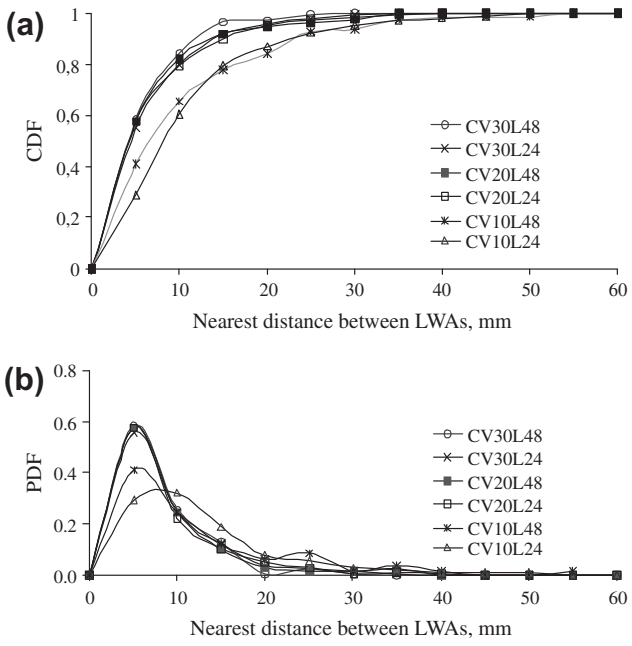

Fig. 6. (a) The cumulative distribution function (CDF) and (b) the probability distribution function (PDF) for a total of 838 LWA–LWA proximities.

Table 2
Results of Powers and Attiogbe mean spacing calculations and the image analysis of the LWA–LWA proximities.

	CV10L24	CV20L24	CV30L24	CV10L48	CV20L48	CV30L48
Number of LWAs, n	66	162	238	40	74	98
Total area of LWAs, mm^2	272	836	1182	295	530	1129
Area fraction of LWAs, %	3.1	9.5	13.9	3	6.2	11.2
Image area, mm^2	8787	8800	8504	9817	8542	10,080
Powers						
$\bar{L}$, mm	43.69	22.38	14.49	57.15	26.31	17.60
Attiogbe						
$\bar{S}_1$, mm	30.58	15.67	10.14	40.00	18.42	12.32
F_v	1.25	2.17	2.86	1.25	2.17	2.86
$\bar{S}_2$, mm	19.16	16.97	14.52	25.06	19.95	17.63
Image analysis						
Average, mm	10.44	6.29	6.25	9.90	6.32	5.47
50th, mm	3.85	3.80	4.25	6.85	3.85	3.75
95th, mm	20.90	19.90	17.55	31.05	20.90	14.45
Autogenous shrinkage strain (28 days), μm/m	−410	−285	−40	−480	−360	−183

where p_v, α_v, A_v, and F_v are the paste volume fraction, specific surface area of LWAs, volume fraction of LWAs, and the fraction of the total paste volume within distance of $\bar{s}$ from the edges of LWAs.

Using image analysis programs (MicroImage and ImageJ), all the LWAs were fitted to ellipses, for which the area, the lengths of major and minor axes and the locations were known. For calculating α_v, the area of each ellipse was divided to its volume assuming that ellipses are represented by ellipsoids in three-dimension. The mean value of α_v for all ellipses was used in calculating the spacing factor.

4.2. Results of image analysis

The cumulative and probability distribution function of the nearest neighbor LWA–LWA proximities are given in Fig. 6a and b, respectively. As expected, the distance of the nearest neighbor of LWAs decreased with the volume of the LWAs. The distance between the nearest neighbors for coarse LWAs was unexpectedly shorter than that of finer LWAs when the replacement ratio of 10% is applied, although at higher volume of replacements the effect of size of LWAs on the LWA–LWA proximities became less significant.

The CDF values corresponding to the 50th and the 95th percentiles of the LWA–LWA proximity distributions were used to provide a comparison with the Powers and Attiogbe spacing factors. The results from the image analyses are given in Table 2.

The estimated results of Powers spacing factor have been found greater than the 95th percentile of the LWA–LWA proximity distribution as also previously stated by Snyder [18]. On the other hand, the Attiogbe mean spacing of $\bar{s}_2$ has been found to be similar to the calculated value of 95th percentile of the LWA–LWA proximity distribution. It is presented in Table 2 that the 95th percentile of the LWA–LWA proximity distribution was in reasonable agreement with the magnitude of autogenous strain at 28 days. Since the LWA–LWA proximity is affected by both size and volume of LWA, variations in autogenous strain results can be evaluated with this proximity. Henkensiefken et al. [27] have also recently investigated the effects of distribution of LWAs on internal curing in a different manner and shown that internal curing was more efficient with better distribution of LWAs, even when the same volumes of water are used.

The results of protected paste volume approach, which were calculated for the 0.5, 1, and 2 mm distances of water release, are shown in Fig. 7. For determining the possible water flow length distance, the experimental rate of mitigation of autogenous strain (i.e. ratio of autogenous strain of internally cured concrete to that of the reference concrete at 28 days) is also compared with the results from protected paste volume approach. The experimental result obtained from the measurements of autogenous strain for each series is shown as asterisk in Fig. 7. The values on horizontal axes for each asterisk denote the possible water flow length distances, and using these values it is possible to estimate the approximate

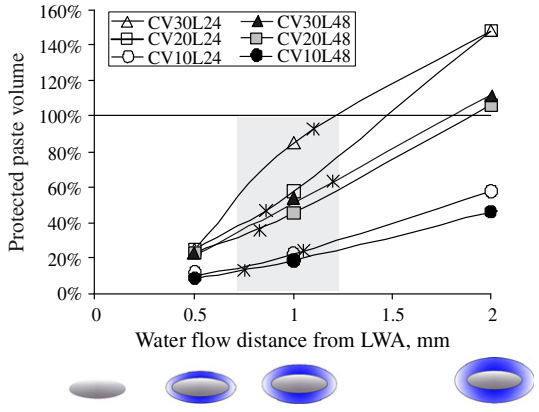

Fig. 7. Fraction of protected paste calculated for variable water flow distance from LWA surfaces. The asterisk on each curve denotes the value of experimentally determined mitigation ratio of each series (from the measurements of autogenous strain).

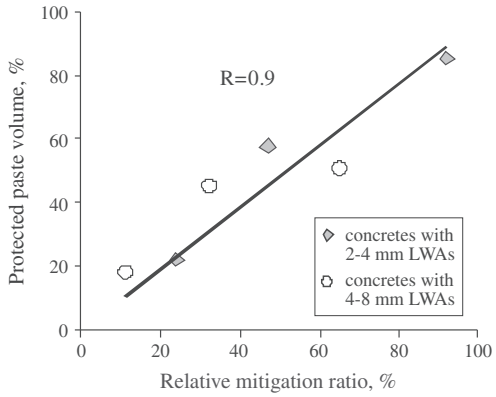

Fig. 8. Comparison of the mitigation ratio of autogenous strain (according to the reference concrete) with the protected paste volume calculated using the water flow distance of 1 mm.

mitigation ratio of autogenous strain. As shown in Fig. 7, the best-fitted values for all concretes with LWAs were found to be water flow of around 1 mm (shown as gray area in Fig. 7) and this is also consistent with the results from water flow experiments presented above. For the replacement by LWAs at high volume fractions, the protected paste volume has been found to exceed 100% for water flow length greater than 1.5 mm. This would require all the cement paste to be protected and even swelling to occur, which has not been observed in the measurements of autogenous strain of concretes tested in this study.

For different series of concrete, the mitigation ratios of autogenous strain with respect to the reference concrete at the age of 28 days were compared with the calculated protected paste volume for water flow length of 1 mm, and a well developed correlation between these values was observed (Fig. 8). Such a correlation indicates that the approximate value of mitigation ratio of autogenous strain in concrete can be estimated by calculating the water-entrained (and therefore internally cured) volume of cement paste using image analysis.

5. Conclusions

On the basis of the experimental work described above the following conclusions can be drawn:

- Experimental results have shown that the use of pre-soaked LWAs as water reservoirs effectively mitigates the autogenous shrinkage of concrete.
- The values corresponding to the 50th and the 95th percentiles of the LWA–LWA proximity distributions can be used to provide comparison with the Powers and Attiogbe spacing factors. The Attiogbe mean spacing of $\bar{s}_2$ was found to be similar to the calculated value of 95th percentile of the LWA–LWA proximity distribution of LWAs. Variation of autogenous strain of concrete can be evaluated with this proximity.
- A well developed correlation between the mitigation ratios of autogenous strain (relative to the reference concrete at 28 days) and the calculated protected paste volume for water flow length of 1 mm has been found. The results indicate that the protected paste volume in internal curing can be determined by image analysis.

Acknowledgements

This research was carried out in the Faculty of Civil Engineering at Istanbul Technical University. The authors acknowledge the grant from DPT (State Planning Organization, Project: 2003K120630).

References

[1] Tanimura M, Mitami Y, Sato R. An investigation of prediction model for autogenous shrinkage/expansion strain of low-shrinkage HSC. In: Persson B, Bentz D, Nilsson L-O, editors. Self-desiccation and its importance in concrete technology proceedings of the 4th international research seminar in Lund; 2005. p. 245–63.
[2] Lam H, Hooton RD. Effects of internal curing methods on restrained shrinkage and permeability. In: Persson B, Bentz D, Nilsson L-O, editors. Self-desiccation and its importance in concrete technology proceedings of the 4th international research seminar in Lund; 2005. p. 210–28.
[3] Hori A, Morioka M, Sakai E, Daimon M. Influence of expansive additives on autogenous shrinkage. In: Tazawa E-I, editor. Proceedings of international workshop autoshrink'98, Hiroshima, Japan, E&FN SPON, London; 1999. p. 187–94.
[4] Bentz DP, Geiker M, Jensen OM. On the mitigation of early age cracking. In: Persson B, Fagerlund G, editors. Self-desiccation and its importance in concrete technology proceedings of the 3rd international research seminar in Lund; 2002. p. 195–204.
[5] Jensen OM, Hansen PF. Water-entrained cement-based materials. I. Principles and theoretical background. Cem Concr Res 2001;31(4):647–54.
[6] Maruyama I, Sato R. A trial of reducing autogenous shrinkage by recycled aggregate. In: Persson B, Bentz D, Nilsson L-O, editors. Self-desiccation and its importance in concrete technology proceedings of the 4th international research seminar in Lund; 2005. p. 264–70.
[7] Mohr BJ, Premenkol L, Nanko H, Kurtis KE. Examination of wood-derived powders and fibers for internal curing of cement-based materials. In: Persson B, Bentz D, Nilsson L-O, editors. Self-desiccation and its importance in concrete technology proceedings of the 4th international research seminar in Lund; 2005. p. 229–44.
[8] Park KB, Noguchi T, Tomosawa F. A study on the hydration ratio and autogenous shrinkage of cement paste. In: Tazawa E-I, editor. Proceedings of international workshop autoshrink'98, Hiroshima, Japan, E&FN SPON, London; 1999. p. 299–308.
[9] Loukili A, Khelidj A, Richard P. Hydration kinetics, change of relative humidity, and autogenous shrinkage of ultra-high-strength concrete. Cem Concr Res 1999;29(4):577–84.
[10] Meshab HA, Buyle-Badin F, Acker P. Early age shrinkage, mechanical behaviour and cracking of fibre reinforced mortar containing recycled aggregates. Concr Sci Eng 2000;2(6):71–7.
[11] Farhat FA, Nicolaides D, Kanellopoulos A, Karihaloo BL. High performance fibre-reinforced cementitious composite (CARDIFRC)-performance and application to retrofitting. Eng Fract Mech 2007;74(1–2):151–67.
[12] Bentz DP, Koenders EAB, Mönnig S, Reinhardt HW, van Breugel K, Ye G. Materials science-based models in support of internal water curing. In: Kovler K, Jensen OM, editors. RILEM report 41 internal curing of concrete, RILEM Publications S.A.R.L; 2007. p. 29–43.
[13] Akcay B, Pekmezci BY, Tasdemir MA. Utilization of artificial lightweight aggregates in hardened cement paste for internal water curing. In: Balazs GL, Borosnyoi A, editors. Proceedings of fib keep concrete attractive, Budapest; 2005. p. 374–80.
[14] Lura P. Autogenous deformation and internal curing of concrete. PhD thesis. Technical University of Delft, Netherlands; 2003.
[15] Müller-Rochholz J. Determination of the elastic properties of lightweight aggregate by ultrasonic pulse velocity measurement. Int J Cem Compos Lightweight Concr 1979;1(2):87–90.
[16] Tasdemir MA. Elastic and inelastic behaviour of structural lightweight aggregate concrete. PhD thesis, Istanbul Technical University, Istanbul; 1982. [in Turkish with English summary]
[17] Akcay B, Tasdemir MA. Optimisation of using lightweight aggregates in mitigating autogenous deformation of concrete. Constr Build Mater 2009;23(1):353–61.
[18] Snyder KA. A numerical test of air void spacing equations. Adv Cem Based Mater 1998;8(1):28–44.
[19] Powers TC. The air requirement of frost-resistant concrete. Proc Highway Res Board 1949;29:184–202.
[20] Philleo RE. A method for analyzing void distribution in air-entrained concrete. Cem Concr Aggr 1983;5:128–30.
[21] Pleau R, Pigeon M. The use of the flow length concept to assess the efficiency of air entrainment with regards to frost durability: part 1– description of the test method. Cem Concr Aggr 1996;18(1):19–29.
[22] Lu B, Torquato S. Nearest-surface distribution functions for polydispersed particle system. Phys Rev A 1992;45(8):5530–44.
[23] Attiogbe EK. Mean spacing of air voids in hardened concrete. ACI Mater J 1993;90(2):174–81.
[24] Attiogbe EK. Predicting freeze–thaw durability of concrete – a new approach. ACI Mater J 1996;93(5):457–64.
[25] Bentz DP, Snyder KA. Protected paste volume in concrete extension to internal curing using saturated lightweight fine aggregate. Cem Concr Res 1999;29(11):1863–7.
[26] Akcay B, Tasdemir MA. Influence of lightweight aggregates on internal curing and fracture of concrete. In: Jensen OM, Lura P, Kovler K, editors. Proceedings of the international RILEM conference, volume changes of hardening concrete: Testing and mitigation, Lyngby, Denmark, PRO 52; 2006. p. 31–40.
[27] Henkensiefken R, Bentz D, Nantung T, Weiss J. Volume change and cracking in internally cured mixtures made with saturated lightweight aggregate under sealed and unsealed conditions. Cem Concr Compos 2009;31(7):427–37.